Marine Geology 424 (2020) 106153

Contents lists available at ScienceDirect

Marine Geology

journal homepage: www.elsevier.com/locate/margo

Storm sequencing and beach profile variability at Hasaki, Japan

Sonja Eichentopf[a,*], José M. Alsina[b], Marios Christou[a], Yoshiaki Kuriyama[c], Harshinie Karunarathna[d]

[a] Department of Civil and Environmental Engineering, Imperial College London, South Kensington Campus, London SW7 2AZ, UK
[b] Laboratori d'Enginyeria Marítima, Universitat Politècnica de Catalunya, 08034 Barcelona, Spain
[c] Port and Airport Research Institute, 3-1-1 Nagase, Yokosuka, Kanagawa 239-0826, Japan
[d] Zienkiewicz Centre for Computational Engineering, College of Engineering, Swansea University, Bay Campus, Swansea SA1 8EN, UK

ARTICLE INFO

Editor: Prof Edward Anthony

Keywords:
Storm sequences
Beach erosion
Beach recovery
Storm power
Beach equilibrium
Sandy beaches

ABSTRACT

Beach profile evolution under storm sequence forcing presents an emerging research topic that has only been investigated at a limited number of sites. The occurrence and effects of storm sequencing on beach profile evolution are studied at Hasaki Beach, Japan, using weekly beach profile and two-hourly offshore wave measurements. During the 25-year study period, the supratidal beach at Hasaki is subjected to long-term accretion and steepening while the shoreline shows a long-term oscillation. In addition, oscillations of the supratidal beach volume and the shoreline at semi-annual and annual intervals are identified, which are largely controlled by the variability of the wave height. Hasaki Beach is subjected to frequent storms that often cluster in sequences, especially during the extra-tropical cyclone season (January to March). The majority of storms and sequences generate erosion of the beach above the low water level but some also lead to recovery. Despite a tendency for storms and storm sequences with larger power to cause more erosion, the present data does not demonstrate increased beach erosion by storm sequences. Following these findings, the tendency of the beach to evolve towards equilibrium and the importance of the antecedent beach morphology are demonstrated.

1. Introduction

Beaches continuously evolve in response to changes in the wave conditions. The wave conditions commonly range between high (storm) and low energy conditions, which have traditionally been associated with beach erosion and beach recovery, respectively. Storms that occur in close succession with limited time for beach recovery between storm events are termed storm sequences, storm groups or storm clusters.These have recently received increased attention due to their potentially enhanced erosive effect compared to individual storms, i.e. storms that are not a member of a sequence (e.g. Cox and Pirrello, 2001; Ferreira, 2002, 2005, 2006; Karunarathna et al., 2014; Lee et al., 1998; Ferreira, 2002). This makes it crucial to further investigate the effect of storm sequences based on high quality morphological and hydrodynamic measurements in order to account for their effect in coastal risk assessments and coastal management practices.

However, there is no consensus on the general effect of storm sequences on beaches and site-specific characteristics have to be taken into account (Eichentopf et al., 2019a). Some studies suggest increased erosion due to storm sequences compared to individual storms, potentially because the beach is more prone to further sediment erosion if it has previously experienced erosion in the sequence (Birkemeier et al., 1999; Karunarathna et al., 2014). Karunarathna et al. (2014) directly linked beach erosion to the power of storms and storm sequences using 30 years of morphological and hydrodynamic measurements at Narrabeen Beach, Australia. They identified larger beach erosion for storm sequences than for individual storms of equivalent power.

In contrast, beach evolution towards equilibrium presents a widely accepted concept in coastal morphodynamics. This has been described in the fundamental beach state model by Wright and Short (1984) and Wright et al. (1985), which has been further elaborated and verified in more recent studies (e.g. Birrien et al., 2018; Davidson et al., 2013; Miller and Dean, 2004; Yates et al., 2009). For equilibrium beach evolution, the antecedent morphology plays an important role because it determines the required change of the beach towards equilibrium under a specific wave forcing as reported from various field investigations (e.g. Coco et al., 2014; Morales-Márquez et al., 2018) as well as from laboratory experiments (e.g. Baldock et al., 2017; Birrien et al., 2018; Eichentopf et al., 2019, 2020). In addition to the antecedent beach morphology, further aspects can influence the equilibrium beach evolution at specific field sites, such as tides (e.g. Coco et al., 2014; Dissanayake et al., 2015), wave direction (e.g. Mortlock et al., 2017) as

* Corresponding author.
E-mail address: sonja.eichentopf16@imperial.ac.uk (S. Eichentopf).

https://doi.org/10.1016/j.margeo.2020.106153
Received 24 July 2019; Received in revised form 12 February 2020; Accepted 12 February 2020
Available online 19 February 2020
0025-3227/ © 2020 The Authors. Published by Elsevier B.V. This is an open access article under the CC BY license (http://creativecommons.org/licenses/BY/4.0/).

well as three-dimensional circulation patterns that can increase erosion and hinder recovery (such as persisting megarips as described in Loureiro et al., 2012).

Evolution of a beach towards equilibrium has also been observed under storm sequence forcing (e.g. Angnuureng et al., 2017; Coco et al., 2014; Morales-Márquez et al., 2018; Vousdoukas et al., 2012). In these studies, the analysis of field measurements did not indicate increased erosion by storms within a sequence compared to individual storms. Results from recent large-scale morphodynamic experiments support these findings (Eichentopf et al., 2020). Eichentopf et al. (2020) observed that the same wave conditions resulted in the same (equilibrium) beach configuration and hence, produced either erosion or recovery of the beach depending on the antecedent morphology.

A major difficulty when studying beach response to sequences of storms is defining storm sequences from the measurements (Eichentopf et al., 2019a). The definition is normally very site-specific, to some extent subjective and ideally, requires long-term measurements. However, morphological and hydrodynamic measurements over multi-annual (decadal) timescales have only been acquired at a few sites around the world (as listed, for instance, in Turner et al., 2016). Consequently, only a limited number of studies have looked into the effect of storm sequences using long-term measurements, such as Lee et al. (1998) and Birkemeier et al. (1999) at Duck, N. C., USA, and Karunarathna et al. (2014) at Narrabeen Beach, Australia. Often, a major limitation of long-term data sets that comprise both beach profile and wave measurements is the insufficient temporal resolution of the profile measurements. This is especially relevant when the profile measurements do not match the storm occurrence as storms usually have an immediate effect on the beach (Eichentopf et al., 2020; Morales-Márquez et al., 2018) that cannot be captured if the pre- and post-storm profiles are measured too long before and after the storm occurrence (Karunarathna et al., 2014).

Despite growing research efforts on storm sequences and beach response, studies that focus on the influence of storm sequences are very scarce and the measurements do not always provide the resolution needed for a detailed analysis. A lack of comprehensive understanding of storm sequencing and beach response hinders the development of coastal management practices that account for storm sequencing. The present study aims to investigate the influence of storm sequences based on long-term (25-year) beach profile and wave measurements at Hasaki Beach, Japan. This involves identifying storm sequences from the available measurements and investigating whether storms within a sequence generate more severe erosion than individual storms of equivalent power or if the beach evolves towards equilibrium, even under quickly alternating storm sequence conditions.

This paper continues with Section 2 describing the field site and the measurements investigated in the present study. The analysis of the data and the results are presented in Section 3 and comprise the long-term beach profile evolution, the definition of storm sequences as well as their role for beach changes, and the investigation of the beach equilibrium evolution. A discussion and conclusions follow in Sections 4 and 5, respectively.

2. Hasaki Beach, Japan

2.1. Field site characteristics

The Hazaki Oceanographical Research Station (HORS) is located at Hasaki Beach in the Ibaraki Prefecture in Japan and is exposed to the Pacific Ocean (Fig. 1). The beach is characterised as a longshore uniform beach (Kuriyama, 2000, 2002) with fine to medium sand (median sediment size of 0.18 mm) (Katoh and Yanagishima, 1995).

The beach is subjected to a wave-dominated, micro-tidal environment with a tidal range of circa 1.4 m. The high (HWL), mean (MWL) and low (LWL) water levels are 1.25 m, 0.65 m and −0.20 m, respectively, based on the datum level at Hasaki (Tokyo Peil −0.69 m) (Kuriyama, 2002). The HWL and the LWL correspond to the mean high water spring and mean low water spring, respectively. Wave conditions comprise both wind sea and swell waves, predominantly from the northeast to easterly directions. The long-term (25 years) mean significant wave height H_s is 1.35 m (with a standard deviation of 0.73 m); the mean significant wave period T_s is 8 s (with a standard deviation of 1.7 s). High energy (storm) wave conditions are generated between September and October by tropical cyclones, and from January to March by frequent extra-tropical cyclones; waves are relatively small from May to June (Kuriyama et al., 2012). Maximum wave heights of tropical cyclones frequently exceed 4 m, whereas maximum wave heights of extra-tropical cyclones typically range between 3.5 and 4 m.

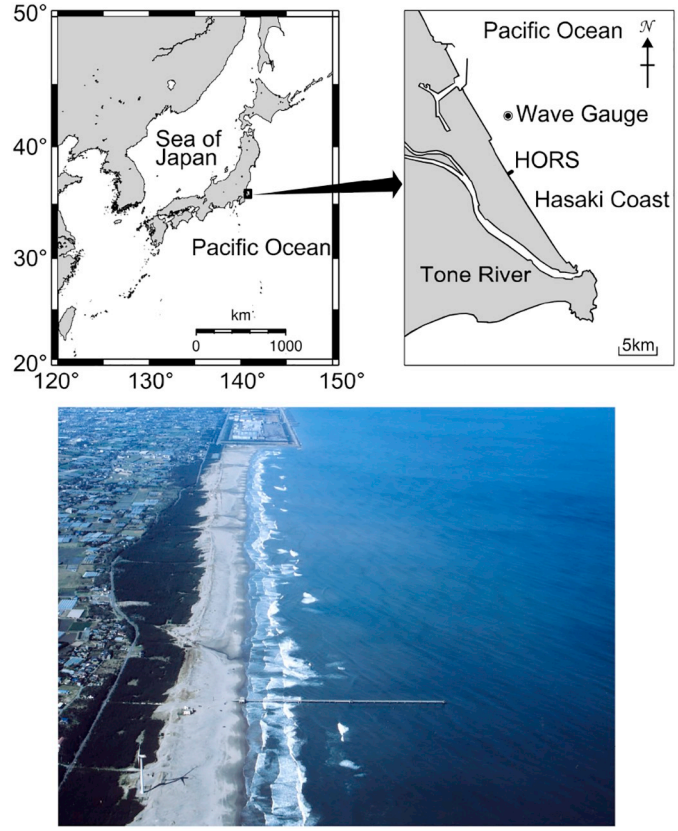

Fig. 1. Study site. Map with location (top panels) and view of the beach with the HORS pier (bottom panel).

2.2. Measurements

The data investigated in the present study involve circa 25 years of beach profile and offshore wave measurements (acquired between March 1986 and December 2010). Beach profiles are measured from the 427 m long HORS pier as well as onshore of the pier resulting in circa 500 m long beach profile measurements with a spatial resolution of 5 m. The pier is supported by single pilings whose influence on the beach profile was investigated in previous studies and reported to be minimal (Kuriyama, 2000, 2002). Due to the uniformity and very long extent of the beach in the longshore direction, profile measurements at one location represent the general characteristics of the beach (Kuriyama, 2000, 2002). The profiles have been measured approximately once a week (on average every 6.92 days with a standard deviation of 0.84 days). The coordinate system used for the profile data in this study is an x-z-coordinate system with x corresponding to the horizontal direction (positive towards the offshore) and z corresponding to the vertical direction (positive upwards). The coordinate system has its origin in x-direction at the most onshore measuring point and in z-direction at the vertical datum of Hasaki.

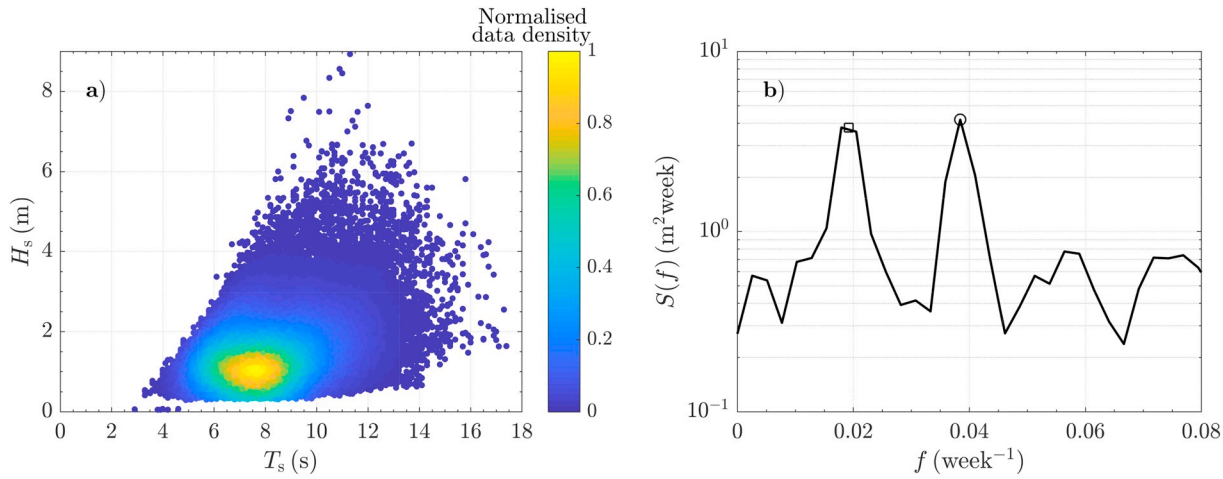

Fig. 2. Incident waves measured for 25 years off Hasaki Coast. a) H_s-T_s scatter plot with colour spectrum indicating the normalised data density. The data density is calculated around each data point and normalised by the maximum data density. b) Spectral density of the detrended H_s signal with square and circle indicating the peaks corresponding to the annual and semi-annual oscillations, respectively.

Deepwater wave data are measured with an ultra-sound wave gauge for 20 min every 2 h at circa 24 m water depth offshore of Hasaki Beach (top right panel in Fig. 1). Gaps in the data were recently filled by Kuriyama and Yanagishima (2018) using linear interpolation of the measurements (if the gaps lasted for less than 24 h) and using data from nearby measuring stations (if the gaps exceeded 24 h). Fig. 2 shows the scatter plot of the significant wave heights H_s and periods T_s as well as the spectral density S of the detrended H_s signal. Fig. 2a shows a concentration of T_s-H_s occurrence at $T_s \approx$ 7–8 s and $H_s \approx$ 1 m, which are close to the long-term mean values of T_s and H_s. The spectral density (Fig. 2b) is plotted against the frequency in units of weeks^{-1} for reasons of comparability against the variability of the beach proxies in the following sections. Two peaks stand out in the H_s spectrum shown in Fig. 2b with peak frequencies that indicate an important annual and a semi-annual oscillation. This may be linked to the aforementioned wave energy variability throughout the year due to annually occurring tropical and extra-tropical cyclone seasons, which are separated by an approximate semi-annual interval (March–October).

3. Analysis and results

Based on the data of weekly beach profile measurements and two-hourly wave records, beach profile evolution and the role of storm sequencing are investigated. Beach profile evolution is primarily studied by means of the mean water shoreline location x_0 (m), i.e. the location of the profile at z = 0.65 m, and the beach volume in different morphodynamic zones. The calculated beach volumes are: the supratidal beach volume V_u (m^3/m) (volume from the most onshore point of the profile measurement to the HWL), the volume of the intertidal zone V_{it} (m^3/m) (volume between HWL and LWL), and the subtidal beach volume V_l (m^3/m) (beach volume below LWL). The shoreline location was calculated at different elevations within the intertidal zone. Differences in the shoreline location were highly consistent over the study duration and peaks in the shoreline power spectrum were very similar (data not shown here).

First, the long-term evolution of the beach profile is presented. Second, a quantitative definition for storms and storm sequences at Hasaki is developed and the influence of storm sequences compared to individual storms is explored. Third, beach evolution towards equilibrium is investigated.

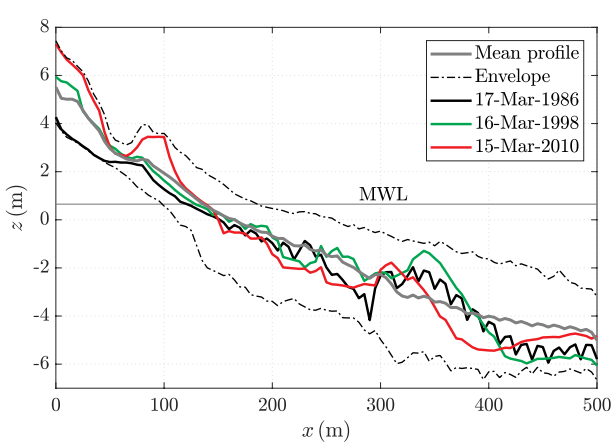

Fig. 3. Mean profile and profile envelope over the 25-year study period. Three example profiles obtained at intervals of 12 years in March are also shown.

3.1. Beach profile evolution

Fig. 3 shows the mean profile and the profile envelope at Hasaki during the 25-year study period. It can be noted that the profiles from 1986, 1998 and 2010 resemble the minimum envelope, the mean profile and the maximum envelope, respectively, very closely in the upper section of the beach (above $z \approx$ 2 m). This provides indication that this upper section of the beach, which makes up a large part of the supratidal beach, is subjected to accretion over the 25-year study period. This is described in more detail below. The supratidal beach is largely affected by winds that can contribute to this long-term trend as was recently investigated by Kuriyama et al. (2019).

To investigate the profile evolution over the 25-year study period, the profile parameters – shoreline location x_0, supratidal beach volume V_u, intertidal beach volume V_{it} and lower beach volume V_l– are calculated for each measured beach profile and are shown in Fig. 4a–d with respect to time. The slope of the supratidal beach, i.e. the slope between the profile at the HWL to the most onshore point of the profile measurement, is also shown (Fig. 4e).

The figure confirms that the supratidal beach (Fig. 4b) is subjected to long-term accretion as indicated by Fig. 3. Steepening of the supratidal beach over time becomes evident (Fig. 4e) and indicates a change of the slope from circa 0.05 ($\approx$ 1/20) in December 1986 to circa 0.06 ($\approx$ 1/16) in December 2010. These trends of increasing V_u and m_u primarily occur due to long-term sediment accumulation at the most onshore part of the measured profiles (see also Fig. 3). Despite these long-term trends, at shorter timescales the volume of the supratidal beach is occasionally marked by reductions of up to 70 m^3/m. This

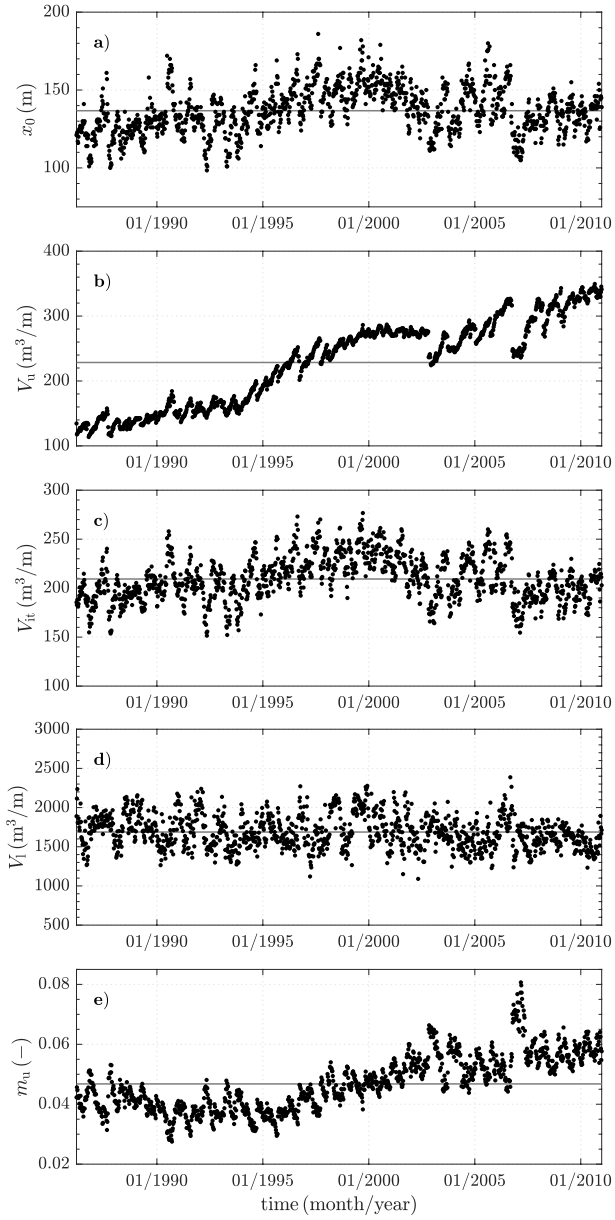

Fig. 4. Time series of beach parameters: a) Shoreline location x_0, b) supratidal beach volume V_u, c) intertidal beach volume V_{it}, d) subtidal beach volume V_l, e) slope of the supratidal beach m_u. Grey thin lines indicate the mean value.

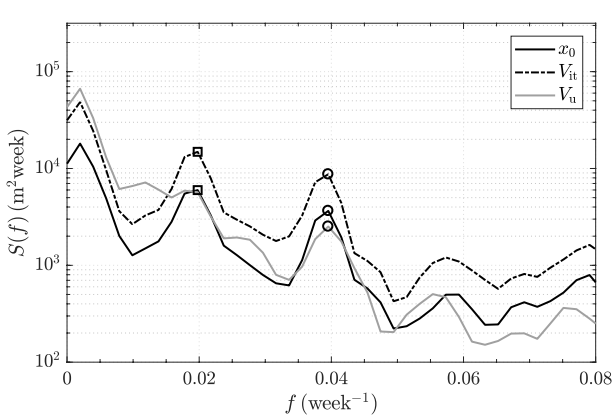

Fig. 5. Spectral density of the shoreline location, the intertidal and the supratidal beach volume from 25 years of profile measurements. Square and circle indicate the peaks corresponding to the annual and semi-annual oscillations, respectively.

sediment is primarily eroded in the lower part of the supratidal beach, i.e. around the HWL, resulting in an increase of m_u.

The shoreline and the intertidal beach volume show a similar pattern with a long-term oscillation and variations at shorter timescales. The similitude between the shoreline and the intertidal beach volume is underlined by their high linear correlation with $R^2 = 0.91$. The volume of the subtidal beach V_l is relatively consistent during the study period oscillating around its long-term mean value of circa 1700m^3/m.

Considering the relevance of the beach above LWL for coastal erosion and flooding as well as the shoreline being a widely used parameter to study beach changes, we will focus on the beach above LWL for the investigation of the effect of storms and storm sequences at Hasaki. It should be noted that the subtidal beach can often experience an increase in sediment volume during high energy waves due to sediment erosion from the supra- and intertidal beach and the formation of nearshore bars.

To investigate the oscillations observed in Fig. 4 in more detail, Fig. 5 shows the spectral density of the detrended signal of the shoreline and the volume of the supratidal and the intertidal beach (using the aforementioned average frequency of profile measurements that had a low standard deviation and was therefore considered applicable for spectral analysis). Fig. 5 indicates peaks in the spectral density at 50.6 weeks (occurring approximately annually) and 25.6 weeks (occurring approximately semi-annually) for the three beach parameters. These are similar oscillation peaks as identified for the H_s spectrum (Fig. 2b), evidencing that the shoreline variability is to a large extent controlled by the variability of the wave height. Fig. 5 also shows a low frequency, i.e. long-term, oscillation, which was already evident for the shoreline and the intertidal beach volume from Fig. 4. Fig. 5 corroborates the similarity between the shoreline and the volume of the intertidal beach as identified from Fig. 4a and c. This similarity can be linked to the fact that the mean water shoreline lies within the intertidal zone.

The timescales of variability can also be related to the medium-term nearshore bar cycle that has been reported for Hasaki (Kuriyama, 2002; Ruessink et al., 2003) although a strong correlation between the bar cycle and the shoreline change has not been confirmed yet. This cycle consists of bar generation close to the shoreline (often associated with shoreline erosion), offshore bar migration through the entire surf zone and bar decay at the offshore end of the nearshore zone (Ruessink et al., 2003). Bar decay has been associated with the onset of a new cycle (Ruessink et al., 2003).

3.2. Defining storm sequence conditions

The quantitative definition of a storm sequence and the associated parameters have been highlighted to be very site-specific (Eichentopf et al., 2019a). Harley (2017) described that a storm can be defined using an offshore significant wave height threshold $H_{s,lim}$, a minimum storm duration D_{min} and the 'meteorological independence criterion' I. The latter refers to the duration for which the wave height can drop below $H_{s,lim}$ without defining a new storm for the subsequent exceedance of $H_{s,lim}$. In the present study, $H_{s,lim}$ is taken as 2.7 m, which is approximately the 95th percentile of the long-term time series of H_s. The 95th percentile intrinsically accounts for the modal wave conditions (Harley, 2017) and has been widely used to determine $H_{s,lim}$ (e.g. Castelle et al., 2015; Splinter et al., 2014).

I and D_{min} are determined as 24 h and 6 h, respectively. Following Harley (2017), I is set to 24 h because Hasaki Beach is subjected to both fast-moving tropical and slower-moving extra-tropical cyclones. H_s was measured every 2 h and therefore, 2 h presents the minimum possible duration of a storm that could be identified from the wave height records. The H_s signal was observed to be of high quality (free of outliers, as also evident from Fig. 2a), however, using D_{min} of 2 h would allow a single H_s value exceeding $H_{s,lim}$ to be identified as a storm. Therefore, 6 h is considered to be a more robust duration to define storms. It ensures that the storm can have an effect on the beach and it is also within

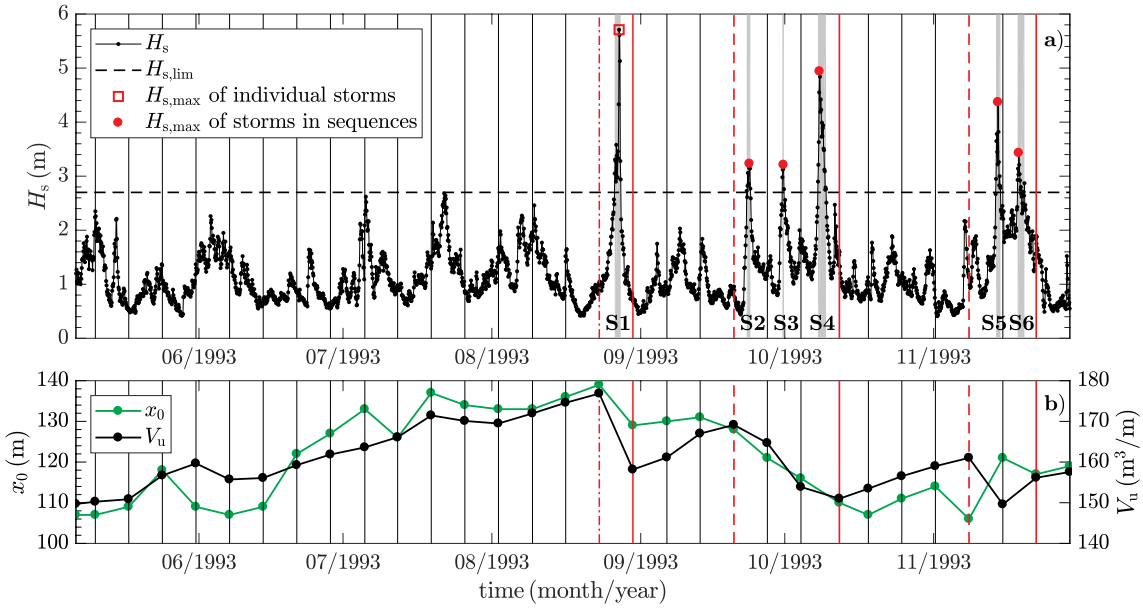

Fig. 6. a) Example section of the H_s time series with identified storms (S1–S6) and storm sequences. Vertical lines indicate dates of beach profile measurements with red dashed (solid) lines corresponding to pre- (post-) profile of either individual storms or storm sequences. b) Shoreline location x_0 and supratidal beach volume V_u of the measured profiles.

the range of storm durations defined for other sites (e.g. Angnuureng et al., 2017; Birkemeier et al., 1999; Karunarathna et al., 2014).

To determine which storms count as individual events and which storms belong to a sequence, a separation time t_r between the storms needs to be defined. Storms that happen within this separation time are considered to form a sequence with the previous storm(s). Starting with the above definition of storms at Hasaki, a combination of visual inspection of the H_s time series, knowledge of reasonable values at other sites as well as a sensitivity analysis of certain parameters (see Section 3.3) were used to determine t_r. Fig. 6a shows an example section of the H_s time series where storms, identified based on the described storm definition, are indicated. Storm events can clearly be noticed with evident peaks of H_s exceeding the storm wave height threshold $H_{s,lim}$. The separation between storm sequences is also evident: while S2, S3 and S4 occur in close temporal succession with circa 7 days between the peaks of the storms, there is a larger time gap between S1 and S2 (circa four weeks) and between S4 and S5 (circa 5 weeks).

Inspecting the entire time series in a similar way as in the example shown in Fig. 6a, a separation time of t_r = 18 days is determined to clearly distinguish individual storms from storms that are a member of a sequence. This choice was further supported by visual observations of beach evolution directly at Hasaki Beach according to which the foreshore needs approximately two to three weeks to recover. This is in line with t_r = 18 days, which was independently defined based on the H_s time series. 18 days represents a standard to large value of t_r compared to other sites (Eichentopf et al., 2019a, Table 1).

Ideally, t_r would be defined using a parameter that provides information on the beach state, such as the shoreline or the beach volume. However, previous studies typically provided little evidence of the recovery happening during the defined thresholds of t_r. It will be further shown in Sections 3.3 and 3.4 that the determination of t_r is not straightforward from beach changes. Despite the site-specific nature of the storm sequence definition, the threshold values determined for Hasaki Beach lie well within a reasonable range compared to other sites (Eichentopf et al., 2019a, Table 1).

Using this quantitative definition for storm sequences, a total of 404 storms were identified within the study period. The majority of the storms (349 storms) make up 94 sequences whereas 55 storms occur as individual storms, i.e. storms that are not members of sequences. 94 storm sequences corresponds to a frequency of 3.8 sequences/year (with a modal value of 3 sequences/year, ranging between 1 and 6 sequences/year). This is a relatively large average frequency compared to other field sites (Eichentopf et al., 2019a, Table 2).

The number of storms within the sequences varies between a minimum of two storms and a maximum of 13 storms. Fig. 7 shows the histogram of the number of storms per sequence. The majority of sequences contain a small number of storms (two to four storms), with a sharp drop for five and more storms per sequence. There is one sequence in each class of 9, 10, 12 and 13 storms presenting large numbers of storms clustering in a single sequence. These sequences normally cover a period of two to three months in the early months of the year, which corresponds to the extra-tropical cyclone season. During this period, storms occur on average every 13 to 14 days (average of all storms in this season over the duration of the season) but can also occur every 5 to 10 days at times. These intervals lie well below t_r = 18 days, which provides an explanation for the large number of storms clustering in sequences during this season of the year.

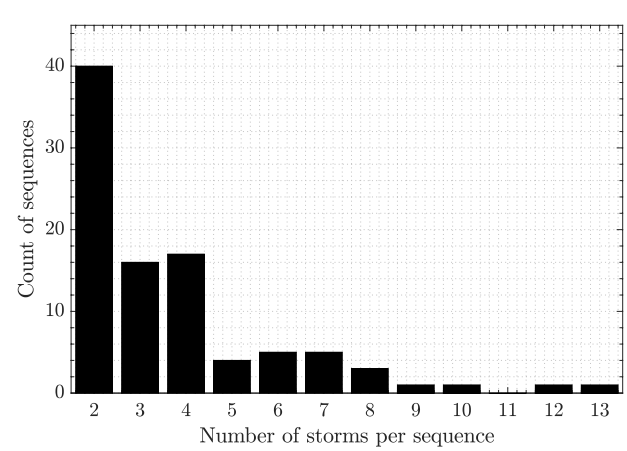

Fig. 7. Histogram of the number of storms per sequence.

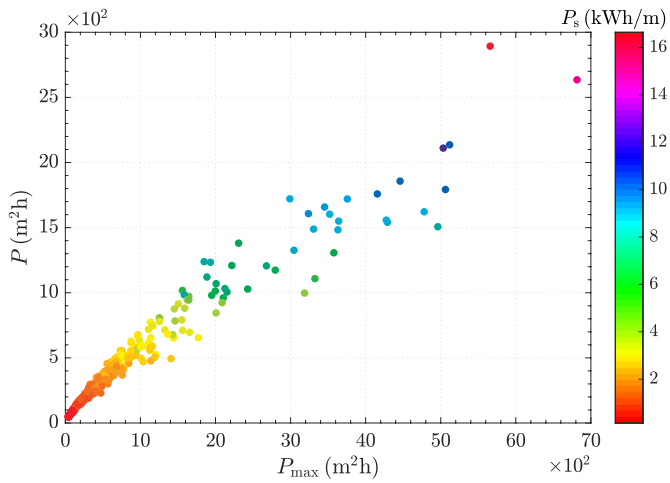

Fig. 8. Comparison of three ways to quantify storm power. Storm power of all identified storms is shown regardless of whether in a sequence or not.

3.3. Effect of individual storms and storm sequences

In this section, we investigate whether storm sequences increase beach erosion at Hasaki Beach. Firstly, the storm power is determined. Secondly, beach changes due to storm sequences are compared to beach changes induced by individual storms. Finally, the sensitivity of the storm sequence definition is investigated.

3.3.1. Power of storms and storm sequences

There are three primary ways to quantify the power of a storm. These are the maximum storm power index $P_{max} = H_{s,max}^2 D$ (Dolan and Davis, 1992, 1994; Karunarathna et al., 2014), the (integrated) storm power index $P = \int_0^D H_s(t)^2 dt$ (Angnuureng et al., 2017; Dissanayake et al., 2015) and the actual storm power $P_s = \int_0^D \frac{1}{64\pi}\rho g^2 H_s(t)^2 T_s(t) dt$ (as used for instance in Eichentopf et al., 2020; Splinter et al., 2014). $H_{s,max}$ is the maximum significant wave height of a storm, D is the storm duration, H_s and T_s are the time-varying storm significant wave height and period, respectively, ρ is the density of water and g is the gravitational acceleration. The power of each identified storm (regardless of whether in a sequence or not) is calculated in these three ways. The results are presented in Fig. 8, which shows that the measures are almost linearly proportional. Linear curve fitting between two of each of the three measures resulted in clear linear relationships with a minimum value of $R^2 = 0.92$. Because of the similar qualitative result of the three parameters, in this work P is used as a relatively simple descriptor for the quantification of the power of storms and storm sequences. It should be noted that P is also directly related to wave energy E through a factor that involves the density of water ρ and the gravitational acceleration g, more specifically $E/P = 16/\rho g$.

Following the above definition for storms and storm power, Fig. 9 presents the storm wave climate at Hasaki. Fig. 9a reveals that the maximum wave height of the majority of storms stays below 6 m but some (all of which are members of storm sequences) lie between 6 m to 8 m and one storm has a maximum wave height of almost 9 m. In terms of the storm duration (Fig. 9b), the majority of storms are relatively short, only a few storms exceed a duration of 80 h and three storms last for circa 200 h. Since P is obtained based on H_s and D of the storms, variations of these two parameters as well as variations in their joint occurrence result in P being spread between circa 40 m^{2}h and 3000 m^{2}h where the majority of storms have a $P < 800$ m^{2}h.

P presents a measure of the power of each identified storm. Considering sequences of storms, the cumulative (or total) power index of a sequence P_{cum} is defined as the sum of P from all storms within the same sequence. Fig. 10 shows the histogram of P_{cum} of the storm sequences. It becomes evident that the majority of storm sequences range within the lower power classes (< 3000 m^{2}h) and only a very limited number of nine sequences exceeds $P_{cum} = 3000$ m^{2}h.

3.3.2. Beach changes due to storms and storm sequences

Fig. 11a,b (left panels) presents the change of the shoreline as well as of the supratidal beach volume against the power index P for the individual storms, i.e. storms that were not members of a sequence. The change of the beach parameters is calculated as the difference between the pre- and post-storm profile. Owing to the high frequency of beach profile measurements, the pre- and post-storm profiles were measured no more than 7 days before (after) the start (end) of each individual storm and hence, the effects of storms on beach profile change can be well captured.

The majority of the individual storms generate shoreline and beach volume erosion but some storms also result in accretion of the beach. A tendency towards increased erosion for larger values of P can be observed for shoreline and beach volume changes but the pattern is not clear as storms with large P (> 1600 m^{2}h) can also produce accretion of the shoreline and almost no change of the supratidal beach volume.

To compare beach changes due to individual storms to beach changes caused by storm sequences, Fig. 11c,d (right panels) shows shoreline and beach volume changes against the total (i.e. cumulative) power index P_{cum} of the storm sequences. The change of the beach parameters is calculated as the difference between the pre- and post-profile of each sequence (measured no more than 7 days before (after) the occurrence of the first (last) storm of each sequence). Similar to the individual storms, the majority of storm sequences generate beach erosion and some tendency towards increased beach erosion for larger

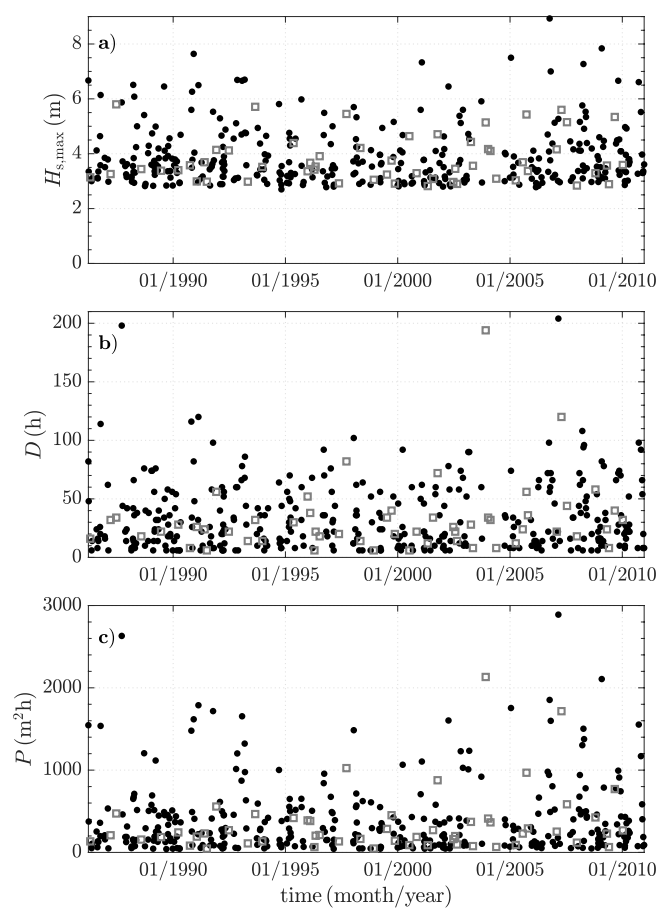

Fig. 9. Storm wave climate at Hasaki. a) Maximum significant wave height $H_{s,max}$, b) duration D and c) power index P of each storm. Solid black circles refer to storms in sequences, hollow grey squares denote individual storms.

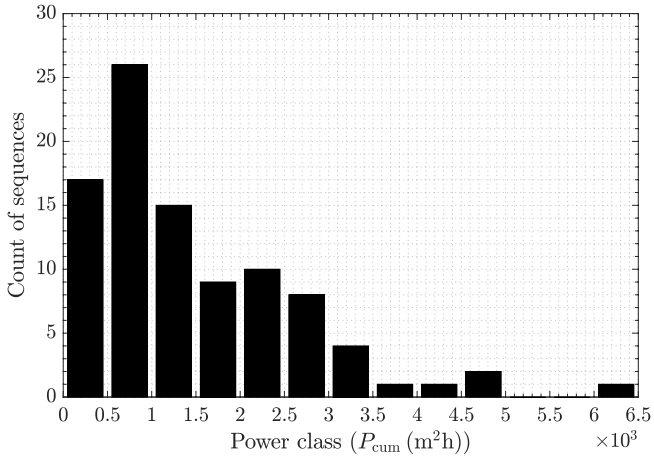

Fig. 10. Histogram of the power classes of the storm sequences.

power can be noted. However, some storm sequences can also generate accretion of the beach, even for relatively large values of P_{cum}.

It should be noted that individual storms do not exceed P of approximately 2200 m^{2}h limiting the comparison of beach changes due to individual storms (Fig. 11a,b) with beach changes due to storm sequences of varying power (Fig. 11c,d). Despite the similar tendency towards increased erosion for larger values of P and P_{cum}, increased erosion due to storm sequences compared to individual storms with the same power is not evident from Fig. 11. Linear best fit lines between changes of the beach parameter (volume or shoreline) and P or P_{cum} had very small values of R^2 (< 0.32). This shows that the storm power alone does not explain beach changes for neither individual storms nor storm sequences.

Fig. 6b shows the evolution of the shoreline and the supratidal beach volume during the example section of the H_s time series (Fig. 6a). Overall, the shoreline and the supratidal beach volume show a similar evolution during the presented section. It can be noted that during the long summer period (almost four months) with H_s below the storm threshold, the shoreline accretes from $x_0 \approx 110$ m to $x_0 \approx 140$ m. The supratidal beach volume also increases from $V_u \approx 150$ m^3/m to $V_u \approx 180$ m^3/m. This highlights the long (weeks to months) timescale that can be required for beach recovery. The accretion of the supratidal beach and the shoreline is largely related to a net sediment movement from the subtidal into the inter- and supratidal zone. This recovery process can occur in stages as recently reported by Phillips et al. (2019) and it is also sometimes associated with welding of an inner bar to the shoreline (Pape et al., 2010; Phillips et al. (2019)).

Overall, both x_0 and V_u show typical periods of erosion and accretion during the following storms and low energy conditions, respectively. However, during the low energy conditions after the sequence of three storms (S2, S3, S4) the shoreline experiences only limited recovery. Therefore, the beach is very narrow at the beginning of the subsequent sequence of two storms (S5 and S6) during which the shoreline recovers. A similar observation is made for V_u: After S5, V_u is very small and the subsequent storm of the sequence S6 leads to accretion of the supratidal beach.

Despite only presenting an example section of circa six months taken from the long-term data set, it becomes evident from Fig. 6b that not all high energy wave conditions generate shoreline erosion, neither do all low energy wave conditions generate shoreline accretion. Fig. 6b as well as Fig. 11 indicate that aspects other than the power index (which is associated with storm wave height and duration) are important in determining whether the beach erodes or accretes under the incident wave conditions. Previous studies have highlighted the importance of the antecedent beach state and the associated availability of sediment for the morphological response to wave forcing (e.g. Baldock et al., 2017; Eichentopf et al., 2020; Grasso et al., 2009; Lee et al., 1998; Morales-Márquez et al., 2018; Scott et al., 2016; Vousdoukas et al., 2012; Yates et al., 2009). The antecedent beach state determines how far the beach is from the equilibrium state that is specific for any given wave condition. This is further investigated in Section 3.4.

3.3.3. Sensitivity analysis of storm sequence parameters

As described in Section 3.2, the definition of storm sequences is site-specific and, to some extent, subjective. In this section, we explore the robustness of the introduced definition of storm sequences by discussing variations of certain parameters.

The time interval t_r between two storms presents the key parameter

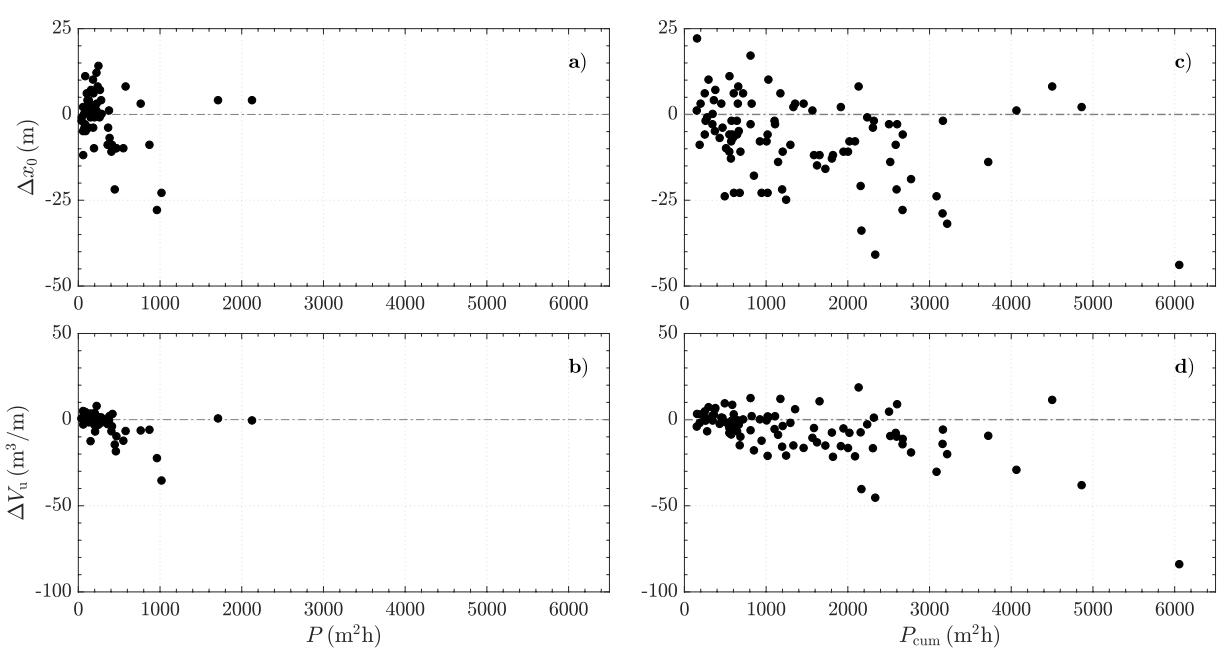

Fig. 11. Change of beach parameters against power index P for individual storms (left panels) and against cumulative power index P_{cum} for storm sequences (right panels). Top panels: shoreline change Δx_0. Bottom panels: change of supratidal beach volume ΔV_u.

to distinguish storm sequences from individual storms. t_r is commonly referred to as "system recovery time", as it is supposed to correspond to the time that the beach needs to fully recover after a storm. However, as previously shown in this section, beach erosion and recovery are not always associated with high and low energy wave conditions, respectively. Therefore, in the present study, t_r is not defined based on the recovery of a beach parameter, such as the shoreline or the beach volume. Instead, t_r is determined based on the identification of temporally clustered storm events in the time series of the wave records and is referred to as "separation time" in the present work.

A further important aspect when defining t_r is a sensible number of sequences occurring at the site and that only a limited number of sequences comprises a very large (> 10) number of storms (see Fig. 7). As aforementioned, the sequences that comprised a large number of storms occurred during the very stormy extra-tropical cyclone season at Hasaki (January to March).

t_r directly determines the number of storm sequences as well as the number of storms that occur in sequences. Fig. 12 shows the variability of the number of sequences and the number of storms in sequences with t_r varying between 12 and 24 days. Note that the total number of storms identified in the 25-year study period was $n_{total} = 404$. n_{total} is a constant when varying t_r, such that $n_{total} = n_{seq} + n_{ind}$ where n_{seq} and n_{ind} denote the number of storms in sequences and the number of individual storms, respectively. Consequently, an increased (reduced) number of storms in sequences results in less (more) individual storms. Generally, a larger t_r results in less storm sequences and more storms counting as a member of the sequences, as it makes previously separated sequences merge in one sequence and previously individual storms to become members of a sequence. On the contrary, a reduced value of t_r results in fewer storms occurring in sequences but not necessarily more storm sequences because storms that previously made up a sequence are separated and then counted as individual storms. Fig. 12a shows that the number of storm sequences is relatively constant between 12 and 20 days and shows a rapid drop for values > 20 days. 18 days lies well within this constant line. The number of storms in sequences gradually grows for increasing t_r (Fig. 12b). The vast majority of storms occur in sequences (even for $t_r = 12$ days) and it would not be sensible for this number to approach close to n_{total}. Moreover, it was found that $t_r = 24$ days resulted in a larger number of sequences with > 10 storms that last for six to seven months. This seems rather unrealistic considering that the extra-tropical cyclone season with frequent storm occurrences lasts for circa three months per year. In addition, the overall pattern of eroded beach volume against total power index of the storm sequences (Fig. 11c,d) was found to be relatively insensitive to changes in t_r varying between 12 days and 24 days.

Variations of I were also examined as I primarily affects the total number of storms (the results are not shown here, main findings are briefly described). Lowering I from 24 h to 12 h resulted in the same number of storm sequences. It generally resulted in a slight shift towards more sequences with > 5 storms, primarily at the expense of sequences with two storms. Increasing I from 24 h to 36 h (in steps of 2 h) had almost no effect on the number of storm sequences or the number of sequences with a large number of (> 10) storms. This supports that, for the studied data, the effect on the storm sequence definition due to variations of I between 12 and 36 h is relatively small.

3.4. Equilibrium shoreline evolution

The previous sections have shown that not all storms cause beach erosion and that not all low energy conditions produce recovery of the beach. It has been postulated that the antecedent beach state is important to distinguish between erosion and recovery for a specific wave condition. This is also evident from Fig. 6b where the second storm (S6) of the sequence of two storms does not generate further erosion of the very narrow beach but, instead, generates shoreline recovery.

Following Yates et al. (2009), who identified the antecedent beach state to be essential for understanding beach changes, Fig. 13 shows the change rate of the shoreline against the initial shoreline location and the wave power index. In the present study, a period of 25 years with weekly beach profile measurements is investigated and oscillations below a semi-annual frequency were identified in the shoreline signal (see Section 3.1). These oscillations occur at longer periods than the typical duration of storms and storm sequences and therefore, are superimposed on the short-term (i.e. at the timescale of storms or sequences) shoreline changes. To compare the shoreline changes due to storms and storm sequences without the influence of low frequency variations, a high-pass filter with a cutoff frequency of 0.045/week (≈ 22 weeks) was applied to obtain the high-pass filtered shoreline signal $x_{0,hp}$. This provided a much clearer distinction between shoreline erosion and accretion than referring to the long-term mean shoreline position.

Fig. 13 evidences that, for the same wave power, $x_{0,hp}$ can either recede or recover depending on its disequilibrium at the beginning of the wave condition. A tendency towards larger shoreline changes for shoreline locations that are further away from their equilibrium state for a given wave condition becomes evident (indicated by darker colours). Fig. 13 compares well with the results in Yates et al. (2009) and Ludka et al. (2015), separating shoreline erosion and accretion depending on the wave energy and initial shoreline location. However, for Hasaki the separation between shoreline erosion and accretion seems to have a larger (negative) gradient, i.e. it is closer to a vertical line, indicating a stronger influence of the initial shoreline location and a

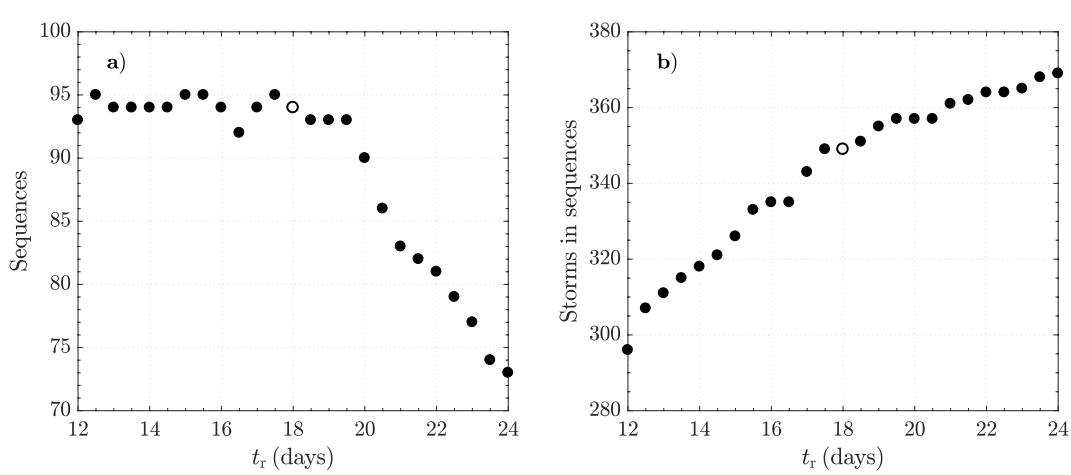

Fig. 12. Sensitivity of storm sequence definition to changes in t_r. a) Number of storm sequences and b) number of storms in sequences depending on t_r. Hollow circles correspond to $t_r = 18$ days used in this study.

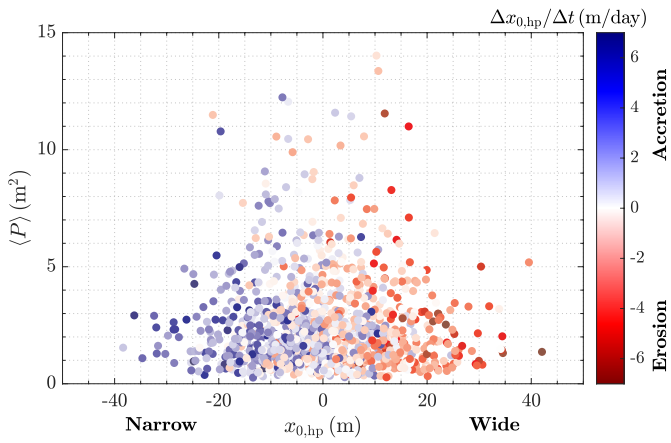

Fig. 13. Shoreline change rate $\Delta x_{0,\mathrm{hp}}/\Delta t$ between weekly measured profiles against the high-pass filtered initial shoreline location $x_{0,\mathrm{hp}}$ and the average power index $\langle P \rangle$ between profile measurements.

lower influence of the wave energy on the shoreline change compared to Yates et al. (2009). It also indicates an overall smaller variability of the high-pass filtered equilibrium shoreline at Hasaki. The equilibrium beach concept also highlights the difficulty of quantifying a "system recovery time" t_r based on beach recovery as it depends on the disequilibrium of the beach for the prevailing wave conditions. In addition, it becomes evident that storm wave conditions can also contribute to beach recovery.

4. Discussion

4.1. Definition of storm sequences

The quantitative definition of storm sequences is site-specific and requires knowledge of the timescale t_r that separates the sequences. In the present study, t_r is not defined based on beach changes as not all low energy conditions between storms recover the beach and not all storms generate erosion. Therefore, t_r is defined from the wave height time series. Previous studies tried to relate t_r to the time that the beach requires to recover its shoreline location or beach volume (e.g. Angnuureng et al., 2017), other studies used a similar approach as in the present study defining a storm sequence as a succession of events based on the wave height time series (e.g. Morales-Márquez et al., 2018; Vousdoukas et al., 2012). These two approaches relate to what Gravois et al. (2018) distinguished as "morphological storm sequence" and "storm sequence in the wave climate". The "morphological storm sequence" accounts for the beach recovery in between storms, whereas a "sequence in the wave climate" is based on the wave records and the beach might not respond with erosion or accretion to storm and low energy conditions, respectively.

Furthermore, it needs to be noted that storm sequence definitions based on long-term wave records use values that are representative of the entire time series but they are not designed to account for peculiarities of each individual storm, whereas this is possible in studies at shorter timescales. For instance, Coco et al. (2014) and Vousdoukas et al. (2012) defined events as storms that did not exceed the defined storm wave height threshold but that lasted for a long duration and/or generated large erosion. Working with long-term data sets, however, the aim is to determine a generic definition that is applied to the entire time series.

4.2. Effect of storm sequences at Hasaki

Increased erosion of the supratidal beach and the shoreline due to storm sequences compared to individual storms with the same power was not observed in the present study. This is different from what has been reported in previous works using long-term morphological and hydrodynamic measurements. Karunarathna et al. (2014), using approximately 30 years of wave and beach profile data from Narrabeen Beach, identified a positive linear relationship between beach erosion and power index for both storms and storm sequences, but with a larger gradient for storm sequences. This indicated more severe beach erosion for storm sequences compared to individual storms with the same power index. For Hasaki Beach, the present study does not derive such a relationship. Moreover, not all storms and storm sequences generate beach erosion but they can also result in accretion of the beach. The limited number of data points in Karunarathna et al. (2014) has to be noted and different site characteristics need to be taken into account. In contrast to Hasaki, Narrabeen Beach is subjected to storms almost all year round, waves are generally more energetic, and the beach has a much steeper foreshore slope (Karunarathna et al., 2016) all of which can promote beach erosion and relate to more dynamic beach changes.

Instead, for Hasaki the beach equilibrium concept was shown to apply at the timescale of individual storms and storm sequences. The antecedent beach morphology is an important factor to be considered for the equilibrium evolution as it influences whether the same wave condition generates erosion or accretion of the beach. This might question the general use of the terms *erosion* and *accretion* (or *recovery*) in relation with high energy and low energy wave conditions, respectively, as also highlighted in recent studies (e.g. Baldock et al., 2017; Biausque and Senechal, 2019; Birrien et al., 2018; Eichentopf et al., 2019, 2020). It also calls for more detailed investigations across a wider range of sites with differing wave and beach characteristics.

Besides the antecedent beach morphology, other aspects can also be relevant for equilibrium beach evolution, such as bar migration and the influence of tides. Bar development near the shoreline for the onset of a new bar cycle can be associated with erosion near the shoreline. On the other hand, bar welding to the shoreline under low energy conditions can importantly accelerate shoreline recovery (Pape et al., 2010; Phillips et al., 2017, 2019). Despite being less dominant in a micro-tidal setting such as Hasaki, the coincident occurrence of storms and high tides can exacerbate shoreline and supratidal beach erosion whereas storms coinciding with low tides can lead to limited erosion of this part of the beach (Coco et al., 2014; Dissanayake et al., 2015).

The equilibrium evolution of the beach is in line with previous studies that explored short-term beach evolution under single sequences at specific field sites (e.g. Coco et al., 2014; Morales-Márquez et al., 2018; Vousdoukas et al., 2012) and in large-scale laboratory experiments (Eichentopf et al., 2020) and it encourages studies on the performance of equilibrium type beach modelling under storm sequence conditions. For the present data, it is important to account for oscillations below the semi-annual interval when studying the beach equilibrium evolution at the timescale of storms and storm sequences as these variations are superimposed on the initial shoreline locations. The weekly shoreline changes are not significantly affected by the semi-annual, annual and long-term variations as the timescale is small compared to the period of these variations. Similarly, the vast majority of storms (storm sequences) lasted for less than two days (four weeks) and therefore, removing oscillations below the semi-annual frequency when calculating beach changes presented in Fig. 11 revealed only small changes in the beach parameters and it did not alter the overall pattern shown in the figure.

4.3. Temporal scale of study

The present study has focused on the effects of storms and storm sequences at an event-scale or sequence-scale. Therefore, the identified beach variations below the semi-annual frequency were filtered when looking into the beach equilibrium evolution at the timescale of storms and storm sequences. In their recent work, Kuriyama and Yanagishima (2018) investigated interannual changes of the beach in the foreshore

and inner transition zone (between $z \approx 0$ m to 3 m). Although at the short-term scale in the present study the beach is found to evolve towards equilibrium, a concentration of wave energy over a few months to years was reported by Kuriyama and Yanagishima (2018) to be capable of inducing a persistent change of the beach state ("regime shift"). Other long-term changes might be related to large-scale atmospheric oscillation patterns, such as the Arctic Oscillation (AO) and the Southern Oscillation Index (SOI) (Karunarathna et al., 2016; Kuriyama and Yanagishima, 2018; Kuriyama et al., 2012). In addition, wind forcing was recently proposed as an important factor for backshore sediment transport at Hasaki (Kuriyama et al., 2019) and found to promote short- and long-term changes beyond the effects of wave events.

4.4. Limitations of the equilibrium concept

For the equilibrium beach concept, the antecedent beach morphology is essential for subsequent beach changes as it determines the extent of the disequilibrium of the beach in relation to the incident wave conditions (Birrien et al., 2018; Eichentopf et al., 2019, 2020; Yates et al., 2009). In addition, Scott et al. (2016) and Biausque and Senechal (2019) reported that some storms can also lead to recovery because a certain level of energy can sometimes be required for the beach to recover. The energy of these storms has the capacity to mobilise sediment that was stranded offshore during previous high energy wave conditions, for instance in the form of nearshore bars (Baldock et al., 2017; Biausque and Senechal, 2019; Dodet et al., 2019; Scott et al., 2016). This might provide a reason for the data points indicating accretion of the narrow beach under intermediate to high energy wave conditions in Fig. 13.

On the other hand, a few data points in Fig. 13 indicate erosion of the narrow beach under low energy wave conditions. This might be linked to sediment that is stranded offshore and cannot be mobilised to contribute towards the recovery of the beach. In this case, low or intermediate energy conditions propagate and break further onshore, which can cause shoreline erosion. This relates to the concept of "morphological hysteresis" as reported early by Cowell and Thom (1994) and studied in detail by Baldock et al. (2017) and Birrien et al. (2018). Baldock et al. (2017) and Birrien et al. (2018) observed continued erosion for reduced wave energy conditions because the sediment of the previously formed bar got stranded resulting in an alteration of the active beach state. For Hasaki Beach, Kuriyama and Yanagishima (2018) highlighted the importance of extreme events that can lead to persistent changes of the beach (e. g. due to an extreme storm in October 2006, which was extreme in terms of the eroded beach volume, storm power and wave height). This means that the beach profile is altered in such a way that it allows the impact of subsequent storms further onshore and to generate larger erosion than expected solely from their power. This is also when storm sequencing can become important and it also highlights the severe effect and hence, importance, of events that have the capacity to persistently alter the beach state.

5. Conclusions

The occurrence of storms and storm sequences and their effect on beach profile evolution was investigated at Hasaki, Japan, using a high-resolution long-term data set of morphological and hydrodynamic measurements. This data set involved 25 years of weekly beach profile measurements and two-hourly offshore wave records. Storm sequences were primarily defined based on the wave records. Beach changes due to storm sequences were compared against beach changes due to individual storms. The results lead to the following conclusions:

- Spectral analysis evidenced that the supratidal beach volume, the intertidal beach volume and the shoreline location oscillate at an annual and a semi-annual interval. These are close to the oscillation intervals of the incident wave height, highlighting a link between the wave energy oscillations and the beach change at these intervals. In addition, the supratidal beach is subjected to long-term accretion resulting in steepening of the supratidal beach.
- Storm sequences are primarily identified based on the wave height time series, independent observations from the beach and knowledge of quantifications of storm sequence parameters at other field sites. Sensitivity analysis showed the robustness of the definition of storm sequences suggested for the present data and variation (within certain ranges) of the parameters to define storm sequences revealed limited effect on the overall tendency of the effect of storm sequences on beach changes.
- A comparison of three methods to quantify storm power revealed a linear relationship between the three methods for the present data. This indicates that each parameter can be used equally well to describe storm power in a qualitative way.
- No clear pattern of increased erosion of the supratidal beach volume and the shoreline due to storm sequences compared to individual storms of equivalent power was identified for the present data. Despite an overall tendency towards larger erosion for more energetic storms and storm sequences, not all storms and storm sequences cause erosion of the beach. In line with that, not all low energy conditions result in beach recovery. This indicates that other aspects, such as the antecedent beach state at the beginning of a storm or storm sequence, rather than only the power are important for beach changes during storms and storm sequences.
- The beach equilibrium concept was shown to hold for this beach at the timescale of storms and storm sequences. The equilibrium concept applies for short-term beach changes and therefore, semi-annual, annual and long-term oscillations, which can be superimposed on the short-term beach changes associated with storms and storm sequences, were filtered. This does not mean that storm sequencing cannot be important as it can have the capacity to alter the beach state, which can happen relatively fast under extreme wave conditions. However, overall the beach strives to reach an equilibrium state, which is in line with previous studies comprising laboratory and field data on beach evolution.

This study has provided evidence of beach evolution towards equilibrium even under the frequent occurrence of closely spaced storm events for a longshore uniform, micro-tidal beach, such as Hasaki Beach. Despite the potentially site-specific character of the findings, the results of this study imply that, rather than only accounting for storm power, the antecedent beach morphology is a key parameter to be accounted for in coastal management practices.

Declaration of competing interest

The authors declare that they have no known competing financial interests or personal relationships that could have appeared to influence the work reported in this paper.

Acknowledgments

We gratefully acknowledge the Ministry of Land, Infrastructure, Transport and Tourism of the Japanese Government and the Marine Information Group of the Port and Airport Research Institute (PARI) for providing the offshore wave data and the staff from the Hazaki Oceanographical Research Station (HORS) for performing the beach profile measurements. SE acknowledges funding from the Department of Civil and Environmental Engineering, Imperial College London. HK acknowledges the support by the UK Research Councils under Natural Environment Research Council award NE/N013573/1, Title CoastWEB: Valuing the contribution which COASTal habitats make to human health and WEllBeing, with a focus on the alleviation of natural

hazards. Finally, we would like to thank the two reviewers for their comments that helped to improve the manuscript.

References

Angnuureng, D.B., Almar, R., Senechal, N., Castelle, B., Addo, K.A., Marieu, V., Ranasinghe, R., 2017. Shoreline resilience to individual storms and storm clusters on a meso-macrotidal barred beach. Geomorphology 290, 265–276. https://doi.org/10.1016/j.geomorph.2017.04.007.

Baldock, T.E., Birrien, F., Atkinson, A., Shimamoto, T., Wu, S., Callaghan, D.P., Nielsen, P., 2017. Morphological hysteresis in the evolution of beach profiles under sequences of wave climates - Part 1; observations. Coast. Eng. 128, 92–105. https://doi.org/10.1016/j.coastaleng.2017.08.005.

Biausque, M., Senechal, N., 2019. Seasonal morphological response of an open sandy beach to winter wave conditions: the example of Biscarrosse beach, SW France. Geomorphology 332, 157–169. https://doi.org/10.1016/j.geomorph.2019.02.009.

Birkemeier, W.A., Nicholls, R.J., Lee, G.-h., 1999. Storms, storm groups and nearshore morphological change. In: Proceedings of the Coastal Sediments '99 Conference, pp. 1109–1122.

Birrien, F., Atkinson, A., Shimamoto, T., Baldock, T.E., 2018. Hysteresis in the evolution of beach profile parameters under sequences of wave climates - Part 2; Modelling. Coast. Eng. 133, 13–25. https://doi.org/10.1016/j.coastaleng.2017.12.001.

Castelle, B., Marieu, V., Bujan, S., Splinter, K.D., Robinet, A., Sénéchal, N., Ferreira, S., 2015. Impact of the winter 2013–2014 series of severe Western Europe storms on a double-barred sandy coast: beach and dune erosion and megacusp embayments. Geomorphology 238, 135–148. https://doi.org/10.1016/j.geomorph.2015.03.006.

Coco, G., Senechal, N., Rejas, A., Bryan, K., Capo, S., Parisot, J., Brown, J., MacMahan, J., 2014. Beach response to a sequence of extreme storms. Geomorphology 204, 493–501. https://doi.org/10.1016/j.geomorph.2013.08.028.

Cowell, P.J., Thom, B.G., 1994. Morphodynamics of coastal evolution. In: Carter, R.W.G., Woodroffe, C.D. (Eds.), Coastal Evolution: Late Quaternary Shoreline Morphodynamics. Cambridge University Press, pp. 33–86.

Cox, J.C., Pirrello, M.A., 2001. Applying joint probabilities and cumulative effects to estimate storm-induced erosion and shoreline recession. Shore Beach 69 (2), 5–7.

Davidson, M.A., Splinter, K.D., Turner, I.L., 2013. A simple equilibrium model for predicting shoreline change. Coast. Eng. 73, 191–202. https://doi.org/10.1016/j.coastaleng.2012.11.002.

Dissanayake, P., Brown, J., Wisse, P., Karunarathna, H., 2015. Effects of storm clustering on beach/dune evolution. Mar. Geol. 370, 63–75. https://doi.org/10.1016/j.margeo.2015.10.010.

Dodet, G., Castelle, B., Masselink, G., Scott, T., Davidson, M., Floc'h, F., Jackson, D., Suanez, S., 2019. Beach recovery from extreme storm activity during the 2013–14 winter along the Atlantic coast of Europe. Earth Surf. Process. Landf. 44, 393–401. https://doi.org/10.1002/esp.4500.

Dolan, R., Davis, R.E., 1992. An intensity scale for Atlantic Coast northeast storms. J. Coast. Res. 8 (3), 840–853.

Dolan, R., Davis, R.E., 1994. Coastal storm hazards. J. Coast. Res. 12, 103–114 (Special Issue: Coastal Hazards).

Eichentopf, S., Karunarathna, H., Alsina, J.M., 2019a. Morphodynamics of sandy beaches under the influence of storm sequences: current research status and future needs. Water Sci. Eng. 12 (3), 221–234. https://doi.org/10.1016/j.wse.2019.09.007.

Eichentopf, S., van der Zanden, J., Cáceres, I., Alsina, J.M., 2019b. Beach profile evolution towards equilibrium from varying initial morphologies. J. Mar. Sci. Eng. 7 (11), 406. https://doi.org/10.3390/jmse7110406.

Eichentopf, S., van der Zanden, J., Cáceres, I., Baldock, T.E., Alsina, J.M., 2020. Influence of storm sequencing on breaker bar and shoreline evolution in large-scale experiments. Coast. Eng. 157, 103659. https://doi.org/10.1016/j.coastaleng.2020.103659.

Ferreira, Ó., 2002. Prediction of the impact of storm groups and their importance in coastal evolution. In: Proceedings of the International Conference on Coastal Engineering '02 (ASCE), pp. 2725–2730.

Ferreira, Ó., 2005. Storm groups versus extreme single storms: predicted erosion and management consequences. J. Coast. Res. 42, 221–227.

Ferreira, Ó., 2006. The role of storm groups in the erosion of sandy coasts. Earth Surf. Process. Landf. 31, 1058–1060. https://doi.org/10.1002/esp.1378.

Grasso, F., Michallet, H., Barthélemy, E., Certain, R., 2009. Physical modeling of intermediate cross-shore beach morphology: transients and equilibrium states. J. Geophys. Res.: Oceans 114. https://doi.org/10.1029/2009JC005308.

Gravois, U., Baldock, T.E., Callaghan, D., Davies, G., Nichol, S., 2018. The effects of storm clustering on storm demand and dune recession at old bar, NSW. In: NSW Coastal Conference, pp. 1–15.

Harley, M., 2017. Coastal storm definition. In: Ciavola, P., Coco, G. (Eds.), Coastal Storms. Wiley Blackwell, pp. 1–21.

Karunarathna, H., Pender, D., Ranasinghe, R., Short, A.D., Reeve, D.E., 2014. The effects of storm clustering on beach profile variability. Mar. Geol. 348, 103–112. https://doi.org/10.1016/j.margeo.2013.12.007.

Karunarathna, H., Horrillo-Caraballo, J., Kuriyama, Y., Mase, H., Ranasinghe, R., Reeve, D.E., 2016. Linkages between sediment composition, wave climate and beach profile variability at multiple timescales. Mar. Geol. 381, 194–208. https://doi.org/10.1016/j.margeo.2016.09.012.

Katoh, K., Yanagishima, S.-i., 1995. Changes of sand grain distribution in the surf zone. In: Proceedings of the Coastal Dynamics '95 Conference, pp. 639–650.

Kuriyama, Y., 2000. Medium-term bar movement and sediment transport at HORS. In: Report of the Port and Harbour Research Institute. 39(4). pp. 51–74.

Kuriyama, Y., 2002. Medium-term bar behavior and associated sediment transport at Hasaki, Japan. J. Geophys. Res. 107 (C9). https://doi.org/10.1029/2001JC000899.

Kuriyama, Y., Yanagishima, S., 2018. Regime shifts in the multi-annual evolution of a sandy beach profile. Earth Surf. Process. Landf. 43, 3133–3141. https://doi.org/10.1002/esp.4475.

Kuriyama, Y., Banno, M., Suzuki, T., 2012. Linkages among interannual variations of shoreline, wave and climate at Hasaki, Japan. Geophys. Res. Lett. 39. https://doi.org/10.1029/2011GL050704.

Kuriyama, Y., Yanagishima, S., Banno, M., 2019. Medium-term morphological change in the backshore. In: Coastal Sediments '19 Proceedings, pp. 1308–1318.

Lee, G.-h., Nicholls, R.J., Birkemeier, W.A., 1998. Storm-driven variability of the beach-nearshore profile at Duck, North Carolina, USA, 1981-1991. Mar. Geol. 148, 163–177. https://doi.org/10.1016/S0025-3227(98)00010-3.

Loureiro, C., Ferreira, Ó., Cooper, J.A.G., 2012. Extreme erosion on high-energy embayed beaches: influence of megarips and storm grouping. Geomorphology 139-140, 155–171. https://doi.org/10.1016/j.geomorph.2011.10.013.

Ludka, B.C., Guza, R.T., O'Reilly, W.C., Yates, M.L., 2015. Field evidence of beach profile evolution toward equilibrium. J. Geophys. Res.: Oceans 120, 7574–7597. https://doi.org/10.1002/2015JC010893.

Miller, J.K., Dean, R.G., 2004. A simple new shoreline change model. Coast. Eng. 51, 531–556. https://doi.org/10.1016/j.coastaleng.2004.05.006.

Morales-Márquez, V., Orfila, A., Simarro, G., Gómez-Pujol, L., Álvarez-Ellacuría, A., Conti, D., Galán, A., Osorio, A.F., Marcos, M., 2018. Numerical and remote techniques for operational beach management under storm group forcing. Nat. Hazards Earth Syst. Sci. 18, 3211–3223. https://doi.org/10.5194/nhess-18-3211-2018.

Mortlock, T.R., Goodwin, I.D., McAneney, J.K., Roche, K., 2017. The June 2016 Australian east coast low: importance of wave direction for coastal erosion assessment. Water 9, 1–22. https://doi.org/10.3390/w9020121.

Pape, L., Kuriyama, Y., Ruessink, B.G., 2010. Models and scales for cross-shore sandbar migration. J. Geophys. Res. 115 (F03043). https://doi.org/10.1029/2009JF001644.

Phillips, M.S., Harley, M.D., Turner, I.L., Splinter, K.D., Cox, R.J., 2017. Shoreline recovery on wave-dominated sandy coastlines: the role of sandbar morphodynamics and nearshore wave parameters. Mar. Geol. 385, 146–159. https://doi.org/10.1016/j.margeo.2017.01.005.

Phillips, M.S., Blenkinsopp, C.E., Splinter, K.D., Harley, M.D., Turner, I.L., 2019. Modes of berm and beachface recovery following storm reset: observations using a continuously scanning lidar. J. Geophys. Res.: Earth 124, 720–736. https://doi.org/10.1029/2018JF004895.

Ruessink, B.G., Wijnberg, K.M., Holman, R.A., Kuriyama, Y., van Enckevort, I.M.J., 2003. Intersite comparison of interannual nearshore bar behavior. J. Geophys. Res. 108 (C8). https://doi.org/10.1029/2002JC001505.

Scott, T., Masselink, G., O'Hare, T., Saulter, A., Poate, T., Russell, P., Davidson, M., Conley, D., 2016. The extreme 2013/2014 winter storms: beach recovery along the southwest coast of England. Mar. Geol. 382, 224–241. https://doi.org/10.1016/j.margeo.2016.10.011.

Splinter, K.D., Carley, J.T., Golshani, A., Tomlinson, R., 2014. A relationship to describe the cumulative impact of storm clusters on beach erosion. Coast. Eng. 83, 49–55. https://doi.org/10.1016/j.coastaleng.2013.10.001.

Turner, I.L., Harley, M.D., Short, A.D., Simmons, J.A., Bracs, M.A., Phillips, M.S., Splinter, K.D., 2016. A multi-decade dataset of monthly beach profile surveys and inshore wave forcing at Narrabeen, Australia. Sci. Data 3 (160024). https://doi.org/10.1038/sdata.2016.24.

Vousdoukas, M.I., Almeida, L.P.M., Ferreira, Ó., 2012. Beach erosion and recovery during consecutive storms at a steep-sloping, meso-tidal beach. Earth Surf. Process. Landf. 37, 583–593. https://doi.org/10.1002/esp.2264.

Wright, L.D., Short, A.D., 1984. Morphodynamic variability of surf zones and beaches: a synthesis. Mar. Geol. 56, 93–118. https://doi.org/10.1016/0025-3227(84)90008-2.

Wright, L.D., Short, A.D., Green, M.O., 1985. Short-term changes in the morphodynamic states of beaches and surf zones: an empirical predictive model. Mar. Geol. 62, 339–364.

Yates, M.L., Guza, R.T., O'Reilly, W.C., 2009. Equilibrium shoreline response: observations and modeling. J. Geophys. Res.: Oceans 114 (9), 1–16. https://doi.org/10.1029/2009JC005359.